Beam-Plasma Instabilities in a 2D Yukawa Lattice

S. Kyrkos,[1] G. J. Kalman,[2] and M. Rosenberg[3]

[1]Department of Chemistry & Physics, Le Moyne College, Syracuse, New York 13214, USA
[2]Department of Physics, Boston College, Chestnut Hill, Massachusetts 02467, USA
[3]Department of Electrical and Computer Engineering, University of California San Diego, La Jolla, California 92093, USA

(Received 14 December 2008; published 5 June 2009)

We consider a 2D Yukawa lattice of grains, with a beam of other charged grains moving in the lattice plane. In contrast to Vlasov plasmas, where the electrostatic instability excited by the beam is only longitudinal, here both longitudinal and transverse instabilities of the lattice phonons can develop. We determine and compare the transverse and longitudinal growth rates. The growth rate spectrum in wave number space exhibits remarkable gaps where no instability can develop. Depending on the system parameters, the transverse instability can be selectively excited.

DOI: 10.1103/PhysRevLett.102.225006 PACS numbers: 52.27.Lw, 52.27.Gr, 52.35.Qz

When a charged particle beam penetrates an equilibrium plasma, an electrostatic instability ensues because of the feedback between the two systems, carried by their respective collective modes. These *beam-plasma instabilities* (BPI) have been studied and well understood for a long time for weakly coupled (Vlasov) plasmas [1,2]. Recently, the question of how strong coupling affects the behavior of the BPI, as well as of the related two-stream instability (e.g., [3]) has arisen in relation to strongly coupled dusty (complex) plasmas. A preliminary study of some of the issues involved has been given in [4]. Several experiments have already explored the effect of externally driven (by a laser beam, for example) particles moving across a plasma crystal. In these experiments amongst other things, the excitation of Mach cones [5], etc., were observed. However, in all these cases, there were only a few individually driven particles: i.e., the essential feature of a coherent beam, with its own collective mode that can couple to the lattice modes, was absent. In the experiment of [6], two counterstreaming half-lattices were generated, ultimately causing the lattice to melt: whether this may be attributed to a two-stream instability is an open question. This Letter addresses a scenario of a two-dimensional (2D) triangular lattice of highly charged grains, penetrated by a weakly coupled, $\Gamma_b = (Z_b e)^2/(a_b T_b) < 1$, tenuous beam of small, heavy grains, with a thermal energy spread T_b; the weak interaction between the beam and the lattice is ensured by the lattice (nominal) plasma frequency $\Omega_p = \sqrt{2\pi (Z_l e)^2 n_l / m_l a_l}$ being well above the similarly defined ω_p of the beam [$a = (\pi n)^{-1/2}$ is the Wigner-Seitz radius, and n is the areal density of the particles; system parameters pertaining to the plasma (lattice) are indicated by subscript l, and to the beam by subscript b]. Both the lattice and the beam are immersed in a polarizable plasma background; thus, the interaction between the particles (both lattice and beam) is taken to be governed by a Yukawa potential with a screening parameter κ, $Z_A Z_B e^2 \phi(r)$, $\phi(r) = (1/r) e^{-\kappa r}$.

Compared to the BPI in a weakly coupled plasma, the interaction of the beam with a strongly coupled lattice brings new physical effects into play: (i) coupling between longitudinal and transverse polarizations that would allow the excitation of transverse electrostatic instabilities; (ii) an anisotropic growth rate spectrum of the instabilities; (iii) sensitivity to the direction of the beam injection; and (iv) the emergence of gaps in the excitation spectrum. It should be noted that the transverse polarizations discussed here are of electrostatic origin, induced by correlations, to be distinguished from transverse electromagnetic instabilities [7] induced by magnetic interaction, which would be much weaker than the ones discussed here.

The goal is now to find the unstable eigenmodes of the coupled beam-lattice system and to use the beam resonance condition between the Doppler shifted beam frequency and one of the lattice modes to determine the domain of wave vectors where they can be excited. In order to study the interaction of a plasma beam with a lattice, we need a formalism that can be adapted to both systems. The Quasi Localized Charge Approximation (QLCA) (for details of the formalism see [8]) has this capability: it describes the system through the collective coordinates $\xi^\mu_{\mathbf{k}}$ and $\eta^\mu_{\mathbf{k}}$, the displacements of the ith particle in the lattice as well as in the beam, respectively, from their equilibrium (for the lattice) or quasiequilibrium (for the beam) positions [9],

$$\xi^\mu_i = \sum_{\mathbf{k}} \xi^\mu_{\mathbf{k}} e^{i\mathbf{k}\cdot\mathbf{x}_i}, \qquad \eta^\mu_i = \sum_{\mathbf{k}} \eta^\mu_{\mathbf{k}} e^{i\mathbf{k}\cdot\mathbf{x}_i}. \tag{1}$$

The interaction between the collective coordinates is represented by $D_{\mu\nu}(\mathbf{k})$, the dynamical matrix whose construction for the lattice as a sum over the lattice sites and for the beam by following the QLCA technique is well-known (see, e.g., [8,10]). The condition $\Gamma_b < 1$ implies that the beam supports a longitudinal mode only and that the interaction within the beam and between the beam and the lattice is through the mean field only: then the fundamental equations for the coupled beam-lattice system be-

 © 2009 The American Physical Society

come

$$\omega^2 \xi^\mu_{\mathbf{k}} = D^{\mu\nu}(k)\xi^\nu_{\mathbf{k}} + \omega_0^2(k)\frac{k^\mu k^\nu}{k^2}\eta^\nu_{\mathbf{k}},$$
$$(\omega - \mathbf{k}\cdot\mathbf{v})^2 \eta^\mu_{\mathbf{k}} = \Omega_0^2(k)\frac{k^\mu k^\nu}{k^2}\xi^\nu_{\mathbf{k}} + \omega_0^2(k)\frac{k^\mu k^\nu}{k^2}\eta^\nu_{\mathbf{k}}. \quad (2)$$

Here, $\Omega_0(\mathbf{k})$ is the frequency of the Vlasov (RPA) plasma mode of the lattice, and $\omega_0(\mathbf{k})$ is the Vlasov plasma mode of the beam,

$$\Omega_0^2(k) = \frac{\bar{k}^2}{\sqrt{\bar{k}^2 + \bar{\kappa}^2}}\Omega_p^2, \qquad \omega_0^2(k) = \Omega_0^2(k)\left(\frac{n_l}{n_b}\right)^{1/2}\frac{\omega_p^2}{\Omega_p^2} \quad (3)$$

where $\bar{k} = ka$, $\bar{\kappa} = \kappa a$, and $\mathbf{v}$ is the beam velocity. The eigenmodes of the *unperturbed* (triangular) lattice are the quasilongitudinal (L) and quasitransverse (T) phonons $\Omega_L(\mathbf{k})$ and $\Omega_T(\mathbf{k})$ (see inset to Fig. 3), the roots of $\|\mathbf{D} - \omega^2\mathbf{I}\| \equiv \Delta(\omega) = 0$ [11,12]. These modes are longitudinal and transverse only for directions of propagation along the principal axes of the lattice (0° and 30°); in general, the polarizations are mixed, although for small k values, the respective longitudinal and transverse polarizations prevail. We seek solutions of (2) for $\delta_m(\mathbf{k}) \approx \omega - \mathbf{k}\cdot\mathbf{v}$ in the vicinity of the unperturbed phonon frequencies $\omega \approx \Omega_m(\mathbf{k}) + \delta_m(\mathbf{k})$ ($m = L, T$) in conjunction with the beam-plasma resonance condition

$$\Omega_m(\mathbf{k}) = \mathbf{k}\cdot\mathbf{v}. \quad (4)$$

The characteristic equation representing (2) in the $\mathbf{k}$-coordinate system (where the 1 axis is along $\mathbf{k}$ and the 2 axis is perpendicular to $\mathbf{k}$), is

$$(\omega_0^2 - \delta^2)\Delta(\omega) - \omega_0^2\Omega_0^2(\bar{D}_{22} - \omega^2) = 0. \quad (5)$$

Here, $\bar{\mathbf{D}}(\varphi) = \mathbf{R}(\varphi)\mathbf{D}\mathbf{R}^{\mathbf{T}}(\varphi)$ is obtained by rotation from the frame where the axes coincide with the symmetry axes of the crystal (where the conventionally defined dynamical matrix $\mathbf{D}$ is obtained) into the $\mathbf{k}$-coordinate system: φ is the angle between $\mathbf{k}$ and the x axis. Equation (5) can now be expanded in the vicinity of $\Delta(\omega) = 0$ as

$$\delta_m(\omega_0^2 - \delta_m^2)\frac{\partial\Delta(\omega)}{\partial\omega}\bigg|_{\omega=\Omega_m} = \omega_0^2\Omega_0^2(\bar{D}_{22} - \Omega_m^2). \quad (6)$$

The two growth rates $\delta_{L,T}$ [associated with the respective L (upper sign) and T (lower sign) modes] are the imaginary parts of the complex solutions of (5), which then satisfy

$$\delta_m(\omega_0^2 - \delta_m^2) = \omega_0^2\Omega_0^2 F_m, \qquad F_m = \frac{(\bar{D}_{22} - \bar{D}_{11}) \mp \sqrt{S}}{\pm 4\Omega_m\sqrt{S}} \quad (7)$$

with the invariant S

$$S = (\bar{D}_{11} - \bar{D}_{22})^2 + 4\bar{D}_{12}\bar{D}_{21} = (D_{11} - D_{22})^2 + 4D_{12}D_{21}. \quad (8)$$

Understanding the properties of the cubic Eq. (7) is crucial in analyzing the instabilities. Its central feature is the formation of regions where there is no solution for δ_m.

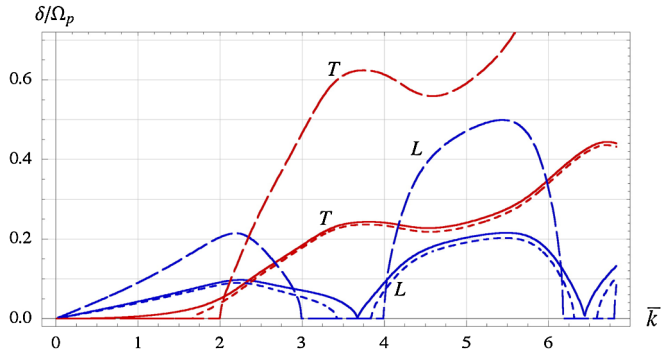

FIG. 1 (color online). $\delta_L(k, \varphi)$ and $\delta_T(k, \varphi)$ as imaginary parts of the complex solutions of (7), for angle $\varphi = 10°$ and $\bar{\kappa} = 2$ [the resonance condition (4) has not yet been applied]. The solid line depicts the case with no linear term in (7) and, consequently, with no gap. The short-dashed lines show the cases $\omega_p/\Omega_p = 0.018$ and the long-dashed for $\omega_p/\Omega_p = 0.18$. The width of the gap grows with increasing ω_p/Ω_p.

Whether this happens is contingent upon the sign of the discriminants

$$\Xi_m = \frac{27}{4}\frac{F_m^2\Omega_0^4}{\omega_0^2} - 1. \quad (9)$$

When Ξ is negative, the cubic equation has three distinct real roots, while when Ξ is positive, it has one real root and a pair of complex conjugate roots. Thus, in the domains of k and φ where $\Xi < 0$, no unstable solutions exist, resulting in gaps in the spectrum of $\delta_{L,T}(k, \varphi)$. These forbidden regions are shown in Fig. 1. For the T mode, they develop

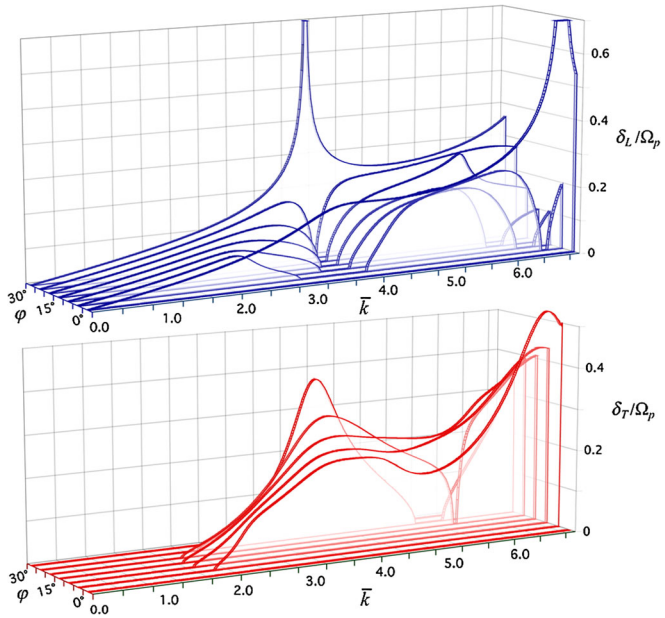

FIG. 2 (color online). Growth rates $\delta_L(k, \varphi)$ and $\delta_T(k, \varphi)$, as solutions of (7), for various angles φ, for $\omega_p/\Omega_p = 0.018$ and $\bar{\kappa} = 2$ [the resonance condition (4) has not yet been applied]. As expected, there is no transverse growth rate when k is along the principal axes of the triangular lattice, i.e., when $\varphi = 0°$ or 30°. Note that the $\varphi = 10°$ graph is also shown in Fig. 1.

for small k values or in the vicinity of the principal axes of the crystal lattice where the two polarizations do not mix much, while for the L mode, they are in the regions of high polarization mixing. Should the linear term in (7) be ignored, its solution would be greatly simplified. The discriminant in that case would be always positive, and no gaps would exist. This is the case in the usual weak coupling (Vlasov) approximation. In reality, the coefficient of the linear term is of the order of $(\omega_p/\Omega_p)^2$. Figure 1 shows how the increase of this parameter affects one of the typical solutions of (7), shown in Fig. 2. The solutions $\delta_m(k, \varphi)$ portray the evolution of the growth rate over the entire **k** space: however, an additional constraint is imposed by the beam resonance condition [with $V = v/(\Omega_p a_l)$ the dimensionless beam velocity and θ its angle of incidence with respect to the x axis]

$$\Omega_m(k, \varphi)/\Omega_p = \bar{k}V\cos(\varphi - \theta) \tag{10}$$

which determines the frequencies $\Omega_m(\varphi; V, \theta)$ and the wave numbers $k_m(\varphi; V, \theta)$ in the vicinity of which the instabilities are generated. The resonance construction is demonstrated in the inset of Fig. 3. Physical solutions result only from portions of the curves that fall outside the shaded forbidden regions. Without loss of generality, $0 < \theta < 30°$ can be assumed, but φ has to run over all the (now inequivalent) Brillouin zones, $0 < \varphi < 180°$. Depending on the value of V (in relation to s_L and s_T, the longitudinal and transverse acoustic speeds, in the same units), and θ, there are three different physical situations, as portrayed in the diagram: (i) $V > s_L$, (ii) $s_L > V > s_T$, (iii) $s_T > V$. Each of them corresponds to a different morphology of the $k_m(\varphi; V, \theta)$ locus in the (k, φ) plane: some typical structures are shown in Fig. 3. It can also be observed that in order to excite instabilities in the physically most interesting small k regions, $V > s_L$ is required. On the other hand, one can selectively excite small k transverse instabilities by choosing $s_L > V > s_T$. The final construction of the growth rates as functions of the wave number k, $\delta_m(k; V, \theta)$, emerges from the combination of (7) and (10). Typical results corresponding to the different scenarios shown in the inset of Fig. 3 are given in Fig. 4; the direction into which the instability is excited, $\varphi_m(k; V, \theta)$, can be read off from the loci in Fig. 3.

The labels L and T, as pointed out above, only identify the modes, but do not represent actual longitudinal or transverse polarizations. Both of the L and T polarization vectors $\hat{\mathbf{e}}_L$, $\hat{\mathbf{e}}_T$, can, however, be decomposed into their longitudinal and transverse components; it is the weights of these decompositions in conjunction with $\delta_{L,T}(k; V, \theta)$ that ultimately determine the actual growths of the longitudinal and transverse electric fields. Such projections, $(\hat{\mathbf{k}} \cdot \hat{\mathbf{e}}_m)^2$, $[1 - (\hat{\mathbf{k}} \cdot \hat{\mathbf{e}}_m)^2]$, for a typical growth rate scenario are shown in Fig. 5.

To see whether experiments to study the BPI discussed in this Letter would be feasible, one has to reconcile: (1) $\omega_0/\Omega_0 < 1$ and $\Gamma_b \ll 1$ requiring low beam density

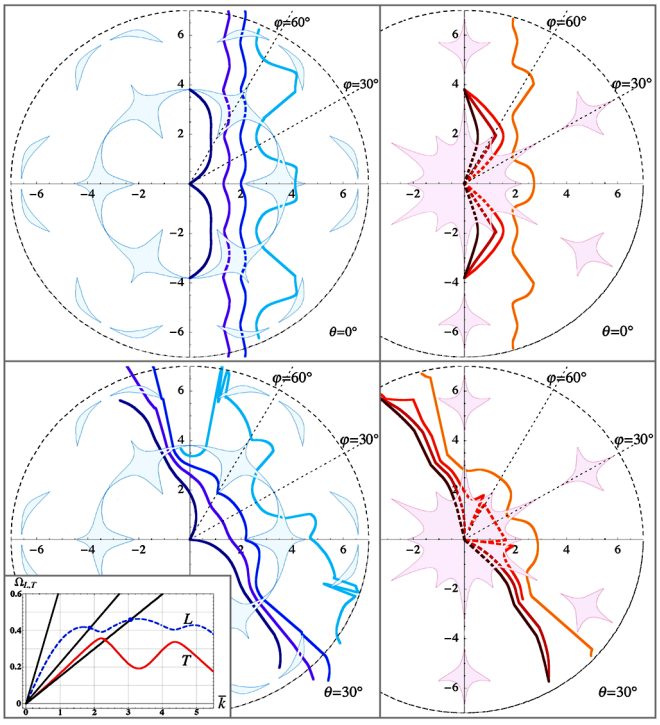

FIG. 3 (color online). Polar diagrams showing loci in the k plane where instabilities can occur, as functions of V and θ, for $\bar{\kappa} = 2$. The left (right) panels pertain to the longitudinal (transverse) instabilities and the upper (lower) panels to $\theta = 0°$ ($\theta = 30°$). The four curves from right to left in each panel correspond to speeds $V = 0.1, 0.2, 0.3, 0.5$. The shaded areas of the background show the locations of the gaps. When the loci fall within the gaps, no acceptable solutions exist for $\delta_{L,T}$. The inset shows the resonance construction for three different values of V in relation to $s_L = 0.16$ and $s_T = 0.41$ [16].

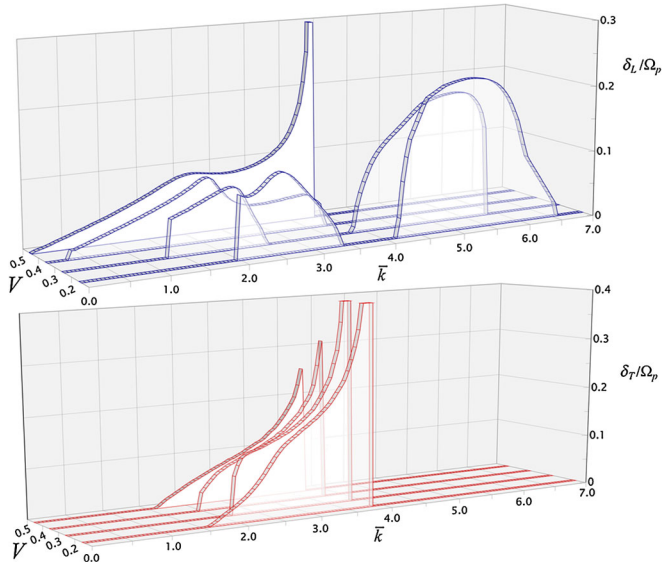

FIG. 4 (color online). Growth rates $\delta_L(k)$ and $\delta_T(k)$ as solutions of (7), with the resonance condition (10) satisfied, for various beam speeds V, for $\omega_p/\Omega_p = 0.018$, $\bar{\kappa} = 2$, and $\theta = 0°$.

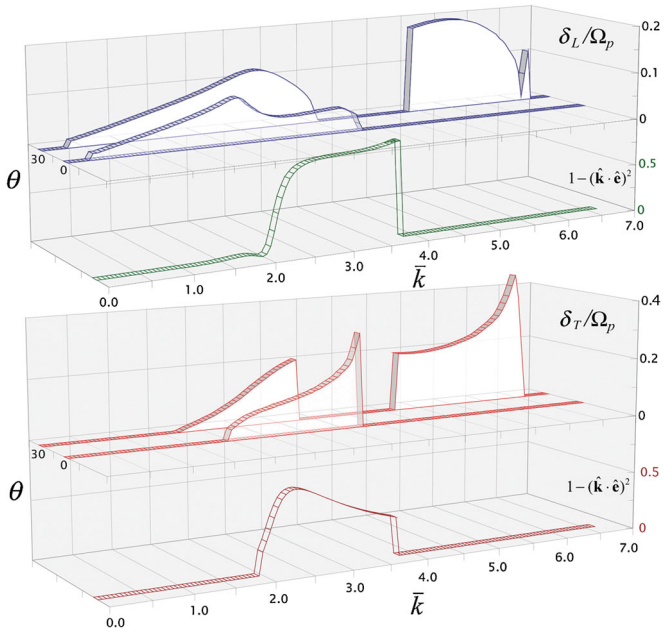

FIG. 5 (color online). Growth rates δ_L and δ_T, as solutions of (7), with the resonance condition (10) satisfied, at angles $\theta = 0°$ and 30° for $V = 0.4$, $\omega_p/\Omega_p = 0.018$, and $\bar{\kappa} = 2$. An example of how the transverse weight is distributed between $\delta_L(k)$ and $\delta_T(k)$ is shown in the bottom part of each panel, where the transverse weight $1 - (\hat{\mathbf{k}} \cdot \hat{\mathbf{e}})^2$ of the respective polarization vectors $\hat{\mathbf{e}}_L$, $\hat{\mathbf{e}}_T$ is portrayed, as a function of k, for $\theta = 0°$.

and beam grains of large mass, (2) beam grains of low kinetic energy (i.e., small mass) in order to minimize effects due to two-body collisions between beam and lattice particles, and (3) low neutral density to ensure small damping caused by grain-neutral collisions. We adopt nominal plasma parameters taken from complex plasma experiments (e.g., [13]), namely, argon gas of pressure $\sim$1 Pa near room temperature, ion density $n_i \sim 3 \times 10^8$ cm^{-3}, and electron temperature $T_e \sim 1$ eV. For the lattice, we consider grains of radius $R_l \sim 3$ μm (grain charge $q_l \sim -5200e$ and using Orbit Motion Limited theory, assuming $T_e \gg T_l$, and a grain surface potential of about $-2.5T_e/e$ [14]), mass density $\sim$1.5 g/cm^3, $a_l \sim$ 200 μm, and T_l near room temperature. For the beam grains, we consider small radius $R_b \sim 0.1$ μm (beam grain charge $q_b \sim -175e$), large mass density $\sim$19 g/cm^3, large $a_b \sim 1$ mm and T_b near room temperature. This yields the following dimensionless parameters: $\Gamma_l \sim 6500$, $\bar{\kappa} \sim 0.5$, $\Gamma_b < 1$, and $\omega_p/\Omega_p \sim 13/96 \sim 0.14 < 1$ $(\omega_0/\Omega_0 \sim 0.3 < 1)$. Estimating the grain-neutral collision frequency ν by using the hard-sphere collision rate (see, e.g., [15]), we find $\nu_l/\Omega_p \sim 0.6/96 \ll 1$ for the lattice, and $\nu_b/\omega_p \sim 1.4/13 \ll 1$ for the beam. With the above parameters, we estimate the longitudinal and transverse sound speeds for the lattice [16,17] as $s_L \lesssim \Omega_p a_l/\sqrt{\bar{\kappa}} \sim 3$ cm/s and $s_T \lesssim \Omega_p a_l/4 \sim 0.5$ cm/s, respectively. Thus, a dust beam with speed $v \sim 2$ cm/s could excite a transverse instability, since $s_T > v > s_L$. The directed dust beam energy would be $\sim$0.2 eV, much smaller than the electrostatic energy between neighboring lattice grains, $\sim$120 eV, indicating the beam may not affect the lattice much via two-body collisions. As to the generation of a dust beam, dust could be accelerated external to the plasma (e.g., by neutral drag) and injected into the plasma. Another possibility may be selective acceleration of nanoparticles by radiation pressure (e.g., [18]). The beam may also be injected above or below the lattice plane to reduce collisional effects.

In summary, we have analyzed the excitation of unstable modes in a 2D lattice of charged grains penetrated by a weak beam. We have identified novel physical effects, such as the selective excitation of transverse instabilities, a gap in $\mathbf{k}$ space and a pronounced anisotropy of the spectrum of the unstable modes, and the sensitivity to the beam injection direction with respect to the principal axes of the lattice. Estimates show that experiments to study these effects should be feasible; they may provide a way to study unexplored phonon spectra arising in more complex situations (binary mixture, bilayers).

This work was partially supported by Grants No. NSF-PHYS 0514619, No. NSF-PHYS 0715227, No. NSF-PHYS 0813153 (G. K.), and No. DE-FG02-04ER54804 (M. R.).

[1] K. I. Golden, G. Kalman, and P. Hammerling, Phys. Lett. A **80**, 149 (1980).
[2] M. Lampe, G. Joyce, and G. Ganguli, IEEE Trans. Plasma Sci. **33**, 57 (2005).
[3] G. Joyce, M. Lampe, and G. Ganguli, Phys. Rev. Lett. **88**, 095006 (2002).
[4] G. J. Kalman and M. Rosenberg, J. Phys. A **36**, 5963 (2003); S. Kyrkos, G. J. Kalman, and M. Rosenberg, IEEE Trans. Plasma Sci. **35**, 342 (2007).
[5] A. Melzer *et al.*, Phys. Rev. E **62**, 4162 (2000); V. Nosenko *et al.*, Phys. Rev. Lett. **88**, 135001 (2002).
[6] V. Nosenko and J. Goree, Phys. Rev. Lett. **93**, 155004 (2004).
[7] Weibel, Phys. Rev. Lett. **2**, 83 (1959); G. Kalman, Nuovo Cimento **20**, 198 (1961); G. Kalman, C. Montes, and D. Quemada, Phys. Fluids **11**, 1797 (1968).
[8] G. Kalman and K. I. Golden, Phys. Rev. A **41**, 5516 (1990); K. I. Golden and G. J. Kalman, Phys. Plasmas **7**, 14 (2000).
[9] M. Rosenberg, G. J. Kalman, S. Kyrkos, and Z. Donkó, J. Phys. A **39**, 4613 (2006).
[10] Z. Donkó, G. J. Kalman, and P. Hartmann, J. Phys. Condens. Matter **20**, 413101 (2008).
[11] S. Zhdanov *et al.*, Phys. Rev. E **68**, 035401(R) (2003).
[12] T. Sullivan *et al.*, J. Phys. A **39**, 4607 (2006).
[13] S. Nunomura *et al.*, Phys. Rev. Lett. **94**, 045001 (2005).
[14] P. K. Shukla and B. Eliasson, Rev. Mod. Phys. **81**, 25 (2009).
[15] M. Rosenberg and G. Kalman, Phys. Rev. E **56**, 7166 (1997).
[16] G. J. Kalman *et al.*, Phys. Rev. Lett. **92**, 065001 (2004).
[17] F. M. Peeters and X. Wu, Phys. Rev. A **35**, 3109 (1987).
[18] A. Ashkin, Phys. Rev. Lett. **24**, 156 (1970).